Journal of Polymer Research (2020) 27: 231
https://doi.org/10.1007/s10965-020-02217-y

ORIGINAL PAPER

Influence of poly(butylene succinate) and calcium carbonate nanoparticles on the biodegradability of high density-polyethylene nanocomposites

Kareem M. Abd El-Rahman[1] · Salah F. Abdellah Ali[1,2] · A.I. Khalil[3] · Sherif Kandil[1]

Received: 10 October 2019 / Accepted: 17 July 2020 / Published online: 22 July 2020

Abstract

The biodegradation is becoming one of the most imperative properties of plastic products nowadays to promote the sustainable development and the conservation of the environment. In this framework, the main objectives of this study are to prepare an environmental friendly high density polyethylene (HDPE) nanocomposite and investigate the effect of the incorporation of nanoparticles of calcium carbonate (NPCC) and poly butylene succinate (PBS) on the prepared nanocomposites. The nanocomposites of HDPE/PBS/NPCC samples were prepared by the addition of PBS and NPCC at (1, 2 and 4 wt%) to HDPE matrix using the injection molding technique. Morphological, mechanical, thermal, physical and biodegradation analysis were conducted on the nanocomposite samples. The mechanical properties of the samples were improved (the elongation at break by 35%, and the impact strength by 26%) compared to the neat HDPE. Moreover, the thermal and physical properties were enhanced by reinforcement NPCC to the nanocomposites. The biodegradation occurrence in the HDPE nanocomposite samples was proved by the Scanning Electron Microscope (SEM) observations and the weight loss percentage (0.265 wt% after 8 weeks).

Keywords High density polyethylene · Biodegradation · Nanoparticles of calcium carbonate · Mechanical properties · *Aspergillus oryaez*

Introduction

During the last few decades, environmental pollution has become a great concern all over the world due to the excessive consumption and accumulation of non-biodegradable plastics which have been deemed as a major source of pollution in the biosphere [1]. The plastic pollution is now clearly observed on land, birds and animals are not far from the consequences as thousands of them were killed due to eating or entangling with plastic products. All of these problems resulted from the ongoing increase of the global plastic waste which was produced over the last seven decades till reached 300 million tons in 2015; reflecting the current waste management pattern and the world production growth of plastics. The plastic annual production thrived more than any other material and exceeded 400 million tons, it is expected to increase by twofold and threefold in 2030 and 2050, respectively.

The majority of the plastic wastes are non-biodegradable thermoplastics synthesized from petroleum resources such as Polyethylene (PE), polypropylene (PP) and polystyrene (PS) [2, 3]. Recently, Polyethylene (PE) is one of the most commonly used polymers, it represents 64% of the thermoplastic products as it comes in many types such as low density polyethylene (LDPE), linear low density polyethylene (LLDPE), high density polyethylene (HDPE) and ultrahigh molecular weight polyethylene (UHMWPE), depending on its density as influenced by the degree of crystallinity [4]. Shedding light

Electronic supplementary material The online version of this article (https://doi.org/10.1007/s10965-020-02217-y) contains supplementary material, which is available to authorized users.

✉ Kareem M. Abd El-Rahman
ch.kareemmahmoud@hotmail.com

✉ Sherif Kandil
s.kandil@usa.net

[1] Department of Materials Science, Institute of Graduate Studies and Research, Alexandria University, El-Shatby, Alexandria 21526, Egypt

[2] College of Science and Arts, Jouf University, Sakaka, Saudi Arabia

[3] Department of Environmental Studies, Institute of Graduate Studies and Research, Alexandria University, El-Shatby, Alexandria 21526, Egypt

on high-density polyethylene (HDPE) as a common commodity polymer that is used in a wide range of applications such as films, packaging containers, bottle caps, toys and household goods. It is a versatile semi-crystalline polyolefin and used extensively due to its low price, availability, recyclability and favorable mechanical and processing properties [5].

High density polyethylene products are very difficult to biodegrade by the action of microorganisms naturally because of its high hydrophobicity [6]. Microorganisms commonly have hydrophilic cell surfaces, which would diminish their ability to colonize on the polyethylene surface and use it as a carbon source. It has been proposed that strains with more hydrophobic surfaces can initiate the colonization on the polymer surface; consequently, the more hydrophobic the bacterial cell surface, the higher the interaction with the polyethylene surface or any other hydrophobic [7, 8]. We selected the filamentous fungus Aspergillus Oryzae to be the biodegradation process host, previous studies stated that this fungus has a hydrophobic cell surface and studied its ability to degrade polyethylene and polyesters such as PSB, PSBA, PCL and PHA [9–11].

Most of the biodegradable synthetic aliphatic polyesters such as polylactic acid PLA, polyhydroalkanoates (PHAs), polycaprolactone (PCL), thermoplastic starch (TPS) and polybutylene succinate (PBS) are capable of degradation by environmental microorganisms. Among these materials, PBS is one of the most successful semicrystalline thermoplastic polyesters that produced from renewable resources and has excellent mechanical properties similar to PE, it also has good elasticity and flexibility more than PLA, higher strength than PBAT (Polybutylene adipate-co-terephthalate), better thermal stability and sensitivity than PCL and high processability. Therefore, PBS and their blends can be used for various potential applications and for the production of environmental friendly biodegradable plastic products in the fields of fiber spinning, textiles, packaging materials, films, mulching film, sheet and injection-molded products [12–14]. PBS also belongs to the hydro-biodegradable polymers group, where the biodegradation process begins with a hydrolysis step at the ester linkages and this results in a reduction of the polymer's molecular weight, allowing further degradation by microorganisms.

The approach will be used in this study is to incorporate a hydro-biodegradable polymer into a non-biodegradable matrix in order to attract the microorganisms to colonize on the surface and form the initial biofilm till they reach the irreversible growth phase; after they are thrived, they would be tricked to use the non-biodegradable molecules as a carbon source leading to a chain cleavage into oligomers and monomers and finally decompose into CO_2, water and biomass [3, 14].

Recently, several studies show that inorganic nanoparticle-filled polymers have unique properties at certain weight percentage (wt%) such as superior mechanical properties, lightweight, barrier properties, toughness and material transparency when compared to neat polymers [15]. Various inorganic nanoparticles, such as nano-clays, nano-talc, nano-SiO_2, and nano-TiO_2, nanoparticles of Calcium carbonate (NPCC) have been added to the polymers composites. Among them, NPCC was widely used in nanocomposites production because NPCC is the cheapest, with commercial availability in readily usable form, easy processability, ability to transfer load by particles with very low aspect ratio, large surface area, and high strength. In general, NPCC can significantly improve the mechanical properties, thermal stability, gas barrier, compatibilization, and morphological properties of the HDPE nanocomposites by achieving an optimized dispersion of the NPCC throughout the HDPE matrix with a good interface at a low wt% of the NPCC (often less than 10% by weight) [15, 16]. This high performance nanocomposites is based on a good dispersion of the nanoparticles in a polymer matrix which is tough challenge because of its higher polar nature and higher surface areas, energy and reactivity with atmospheric moisture, it tends to strongly agglomerate [16, 17]. To increase the particles dispersion and compatibility in the HDPE matrix, the surface of NPCC has been modified by stearic acid. It was found that, Surface treatment of NPCC have better influence on the mechanical properties of the nanocomposite than untreated NPCC [16]. Bartczak, Argon and Cohen [18, 19] prepared HDPE composite with improved mechanical properties compared to virgin PE which depends strongly on the inorganic rigid particles. They discussed that rigid particles could act as stress raisers leading to debonding/voiding and deformation of the matrix around the calcium carbonate that introduced massive number of stress concentration sites in the polymer matrix and promoted cavitations at the particle matrix boundary, these cavities released the plastic constraint and triggered large scale plastic deformation of the composite matrix by the coalescence of the micro-voids [20]. Thus, the massive crazing across the whole gauge length and fracture energy was consumed and then the toughness of matrices such as HDPE or PBS composites filled with NPCC was improved.

To the best of our knowledge, this is the first investigation of modified HDPE with the synthetic aliphatic polyester PBS and NPCC. The objective of the present study is to investigate the influence of incorporating a biodegradable polyester such as PBS and nano particles calcium carbonate on the mechanical, thermal and physical properties, also to study the nanocomposites potentials to biodegrade by the action of microorganisms in a controlled environment.

Experimental

Materials

Injection molding grade of HDPE (HD6070) with a melt flow index of 7.5 g/10 min at (190 °C, 2.16 Kg) and a density of 0.960 g/cm^3 was supplied by Sidi Kerir Petrochemicals

Company, Egypt. HDPE in the form of virgin powder was obtained from the output line of the polymerization reactor without any additives. Nano particle of Calcium Carbonate (NPCC) grade (SN-5300) was provided by Fujian Sannong Calcium Carbonate Co. Ltd., China, with a particle size range of 20–30 nm and cubic shape as shown in Fig. 1, its surface area is 17 m^2/g and was pre-treated with stearic acid. Poly (1, 4-butylene succinate), extended with 1, 6-diisocyanatohexane (PBS) was supplied by Sigma – Aldrich Co. Ltd., UK. With a melt flow index of 10 g/10 min at (190 °C, 2.16 Kg) and a density of 1.3 g/ml at 25 °C and melting temperature 120 °C. The fungus Aspergillus oryzae (ATCC-56747) was used for biodegradation test of plastics. It was obtained from the Microbiological Resources Center (MIRCEN), Cairo, Egypt. This fungal strain was grown on Potato Dextrose Agar (PDA) plates and slants for 7 days at 28 °C and stored at 4 °C.

Preparation of HDPE/PBS/NPCC Nanocomposites

The powder of neat HDPE, NPCC and the pellets of PBS were initially dried in an oven at 60 °C for 24 h to remove any moisture before use. The raw materials were allowed to cool down to room temperature in a desiccator prior to processing. A two-level central composite rotatable design of (PBS wt% and NPCC wt%) was used to investigate the effect of PBS content and NPCC content with different weight ratios (1.0, 2.0 and 4.0 wt%) as shown in Table 1, on the properties of the HDPE/PBS/NPCC nanocomposites. These components of each composite were mechanically mixed using Robot Coupe Blixer 4 Mixer for 6 min with speed 3000 rpm to obtain a well distribution of the additives through the powder matrix. HDPE/PBS/NPCC nanocomposites were molded using an Allrounder 221 k injection molding machine (Arbourg, Germany) with a single screw. Barrel temperatures were set at (T1: 185 °C, T2: 185 °C, T3: 190 °C, T4: 190 °C and T5: 190 °C) from feed section to nozzle, respectively. The screw speed was (90 cm/s) at an injection press of (1300 bar) and the cooling time was (3 Sec).

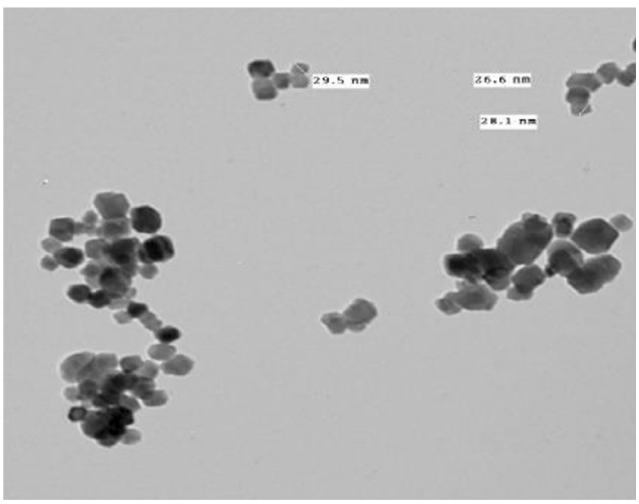

Fig. 1 Nano particles calcium carbonate (NPCC) investigated by Transmission Electron Microscopy (TEM) (JEOL 100cx – USA)

Preparation of the plastic discs for biodegradation test

Plastic discs of the selected sample (A0) as a reference and the blank (A11) were prepared with dimensions of (2.0 × 2.0 × 0.05 cm) by using the hydraulic hot press (SPECAC, USA) with load 5 tons for 8 min at temperature 150 °C. The specimens were dried in a conventional oven at 50 ± 0.5 °C for 24 h, cooled in a desiccator, immediately weighed to the nearest 0.001 g.

Preparation of the biodegradation medium

Fungal minimum medium (FMM), was used. The composition was modified from the Czapek-Dox, a generally used synthetic minimal medium for the fungi Aspergillus oryzae (0.2% $NaNO_3$, 0.1% K_2HPO_4, 0.05% $MgSO_4.7H_2O$, 0.05% KCl, 0.001% $FeSO_4.7H_2O$), pH 7.3 (Koitabashi et al. (2012) [21].

Characterization of the chemical structure of nanocomposite samples

Fourier transform infrared (FTIR) spectroscopy (Nicolet avatar 330 FT-IR, USA) was used to record the FTIR spectra of neat HDPE, HDPE/NPCC, HDPE/PBS and HDPE/PBS/NPCC composites. The samples were scanned in the range from (4000–400 cm^{-1}), and the resolution was 4 cm^{-1} and the average of 16 scans was calculated to determine each FTIR spectrum.

Morphology characterization of nanocomposite samples

Scanning Electron Microscopy (SEM; JEOL, JSM-5300, Japan) was used to monitor the surface and cross section morphology of the neat HDPE, and its nanocomposite samples at an accelerated voltage of 25 KV. The fractured surfaces of the specimen were sputter-coated with a thin layer of gold palladium 400A° by a sputter-coating unit (SPI-MODULE) to obtain better visibility and prevent electrical discharge.

Characterization of the mechanical properties of nanocomposite samples

Tensile properties of the neat HDPE and its nanocomposites were measured according to the ASTM D-638 using the universal testing machine (Zwick/Z005, Germany), with 5 kN load cell and a crosshead speed of 20 mm min^{-1} at the lab

Table 1 The matrix design, name and levels used for nanocomposites of HDPE/PBS/ NPCC

Sample name A (PBS wt%: NPCC wt%)	Actual level of variables		
	HDPE (wt%)	PBS (wt%)	NPCC (wt%)
A0 (neat powder)	100	0	0
A01	99	0	1
A02	98	0	2
A04	96	0	4
A10	99	1	0
A11	98	1	1
A12	97	1	2
A14	95	1	4
A21	97	2	1
A22	96	2	2
A24	94	2	4
A41	95	4	1
A42	94	4	2
A44	92	4	4
A 6070 (HD6070 UA pellet)	100	0	0

conditions 23 ± 2 °C and relative humidity of 50 ± 5%. Tensile strength at yield and Elongation at break (%) were determined and averaged for at least three tensile specimens of type IV that were cut longitudinally from the recently prepared samples.

Impact strength of the neat HDPE and its nanocomposites was evaluated using (CEAST, Germany) impact test machine according to ASTM standard D 4812 -UN notched, which was used to measure the resistance to breakage by flexural shock of plastics. This was indicated by the energy absorbed through standardized pendulum-type hammers, with one pendulum swing. All specimens were conditioned prior to testing at lab conditions for 24 h and were tested at room temperature and relative humidity that were 23 ± 2 °C and 50 ± 5%. Five samples were fitted carefully to the test to shock with hammer load 7.5 J.

Characterization of the thermal properties of nanocomposite samples

The melting temperature (Tm) and the degree of crystallinity (Xc) of neat HDPE, HDPE/ PBS/ NPCC composites were determined by using a Differential Scanning Calorimeter (DSC Netzsch DSC 214, Germany). The samples weights between 5 and 8 mg were sealed in aluminum pans. Each sample was subjected to a heat cycle, it started at lab temperature (24 °C) and cooled to −30 °C using liquid nitrogen at a rate of 10 °C/min and kept for 5 min, then heated till 200 °C at a rate of 10 °C/min and cooled back to −30 °C and kept for 5 min, this step was performed to erase the sample thermal history. After then, the sample was reheated to 200 °C at the same rate, the whole cycle was conducted according to the standard operation procedure (SOP) of Netzsch DSC 214. The degree of crystallinity (Xc %) was auto-calculated using the heat enthalpy of fusion for the samples. According to the following Eq. (1)

$$Xc\% = \left({}^{\Delta Hm}\!/_{\Delta H^{\circ}m} \right) \times 100 \quad (1)$$

Where, (ΔHm) the experimental heat of fusion of the sample (J/g), is the heat consumed for melting, and calculated from the area under the melting peak [22], (ΔH°m) is the heat of fusion value of 100% crystalline HDPE (292.6 J/g) [23].

The change in the weight of a material was determined by Thermogravimetric analysis (TGA) as a function of temperature or time in controlled nitrogen atmosphere [4]. The thermal stability was examined by using Thermogravimetric Analyzer model TGA-50H (Perkin & Elmer- USA) according to (ASTM D 3850–94) for the neat HDPE and its nanocomposite samples. The TGA curves were obtained by heating the samples in the range of (25 to 600 °C) under nitrogen atmosphere at a heating rate of 10 °C min^{-1}, using samples weight of (5 to 9 mg) in a platinum cell.

Characterization of the physical properties of nanocomposite samples

The melt flow index (MFI) of the neat HDPE and HDPE/PBS/ NPCC nanocomposites was determined using (Zwick M flow, Germany) Polymer test melt indexer, at 2.16 kg and 190 °C

indexer, which expresses how many grams of the polymer melt can pass in a die with a width of 2 mm and length 8 mm per 10 mins according to the ASTM D-1238 standard test method. To measure the degree of whiteness (WI) of the neat HDPE and HDPE/PBS/NPCC nanocomposites samples, the colorimeter (Konica Minolta CM-700d/600d, Japan) was used according to ASTM E- 313. The Whiteness Index is a single number ranging from 0 to 100. L* a* b* color system parameters which Lightness (L*) and chromatic coordinates (a*, b*) were measured for 5 replicate samples. L* is widely known as the reflecting diffuser and the maximum L* represents (whiteness) of a perfect reflecting diffuser and the minimum value L* is 0, which represents black. a* and b* have no numerical limit. A positive a* indicates red and the negative one refers to green. The positive b* is yellow and the negative one is defined as blue. Thus, only L* and b* are enough for indicating the coloration and give whiteness index of the HDPE and its composite samples [24].

Biodegradation test

The biodegradation of plastic discs by the microbial attack using liquid flask culture technique was assessed by determining the weight loss and observation of surface morphology changes by using the scanning electron microscope (SEM).

The plastic discs samples of neat HDPE A0, and HDPE composite A11 (pre-weighed and disinfected) were aseptically transferred to 250 ml conical flask containing 100 ml of fungal minimum medium. Then, the flask was inoculated with an identified degrading Microorganism (Aspergillus oryzae) using 2 strips (diameter in 0.5 mm) of 7 days old culture from PDA plate by a sterile cork borer. All the flasks were containing 100 ml of minimum medium (without carbon source) and plastic discs. The sample A0 was used as a control. The flasks were incubated with occasional shaking on a rotary shaker at 28 ± 1.0 °C, 120 rpm. Flaks were checked in schedule (0, 2, 4, 6 and 8 weeks), the plastic discs were collected, washed thoroughly using distilled water, dried at (50 ± 0.5 °C for 24 h) and then weighed [25, 26]. Duplicates were used for each time interval. Finally, the weight loss % was calculated and compared based on the following formula Eq. (2):

$$\textit{Weight loss}\ (\%) = \frac{(\textit{Initial weight} - \textit{Final weight}) \times 100}{\textit{Initial weight}} \quad (2)$$

The morphological features changes of the plastic surface disc of the control sample (A0) and the nanocomposite samples (A11) and the filamentous fungi (Aspergillus oryzae) after incubation were compared by scanning electron microscopy (SEM; JEOL, Japan JSM-5300), at an accelerating voltage of 25 kV. Plastic samples surfaces were dried and coated with gold prior to examination. The coated samples were observed to identify the surface topographical changes after 8 weeks due to microbial degradation and the microbial growths on the surface of the samples.

Statistical analysis of the data

Data were fed to the computer and analyzed using IBM SPSS software package version 20.0. ANOVA, it was used to compare different four sub-groups (A0, A1i, A2i, and A4i), each of which was compared to all of the other samples and followed by Post Hoc test (Tukey) for pairwise comparison.

Results and discussion

Surface morphology using scanning electron microscope (SEM)

SEM was used to investigate the morphological feature, phase behavior and the possible interfacial interaction between the components of nanocomposites and to evaluate the dispersion of NPCC in such composites. Figure 2 shows that HDPE/PBS/NPCC composites that contain a small amount of NPCC (1 wt%) has a good dispersion of the nano particles in the HDPE matrices. It was clearly seen especially in the sample (A11) that it has the best dispersion in the HDPE matrix over all different composites. This uniform dispersion may be attributed to a strong interfacial adhesion between the NPCC and polymer matrix, which can be achieved by surface modification of the NPCC by stearic acid and small wt% of PBS which has high interfacial tension with HDPE phase [17]. Generally, NPCC nanoparticles are hydrophilic and highly polar, whereas many common polymers such as HDPE are nonpolar and hydrophobic. Consequently, NPCC particle surfaces are often modified for better compatibility and adhesion with NPCC and the HDPE matrix, because HDPE reacts readily with fatty acids (stearic acid) and their NPCC. Then NPCC acted as an internal lubricant in the matrix and has significantly improved the mechanical property of the composite [17, 27, 28]. However, at higher content of the NPCC and PBS in HDPE/PBS/NPCC composites more than 1 wt%, some agglomerated NPCC, cavities emerged on the surface of HDPE composites, and it was coarsened with increasing the NPCC and PBS wt%. These observations indicate a poor dispersion and weak interfacial interaction between the agglomerated NPCC and the HDPE matrix as reported previously [16]. When NPCC was increased in the polymer matrix more than the optimum wt%, the dispersion becomes a severe problem, because the nanoparticles of CaCO3 have a strong tendency to agglomerate, because of their high polar and surface energy, which is a result of the small particle size. The aggregated particles have a poor compatibility with the PE matrix,

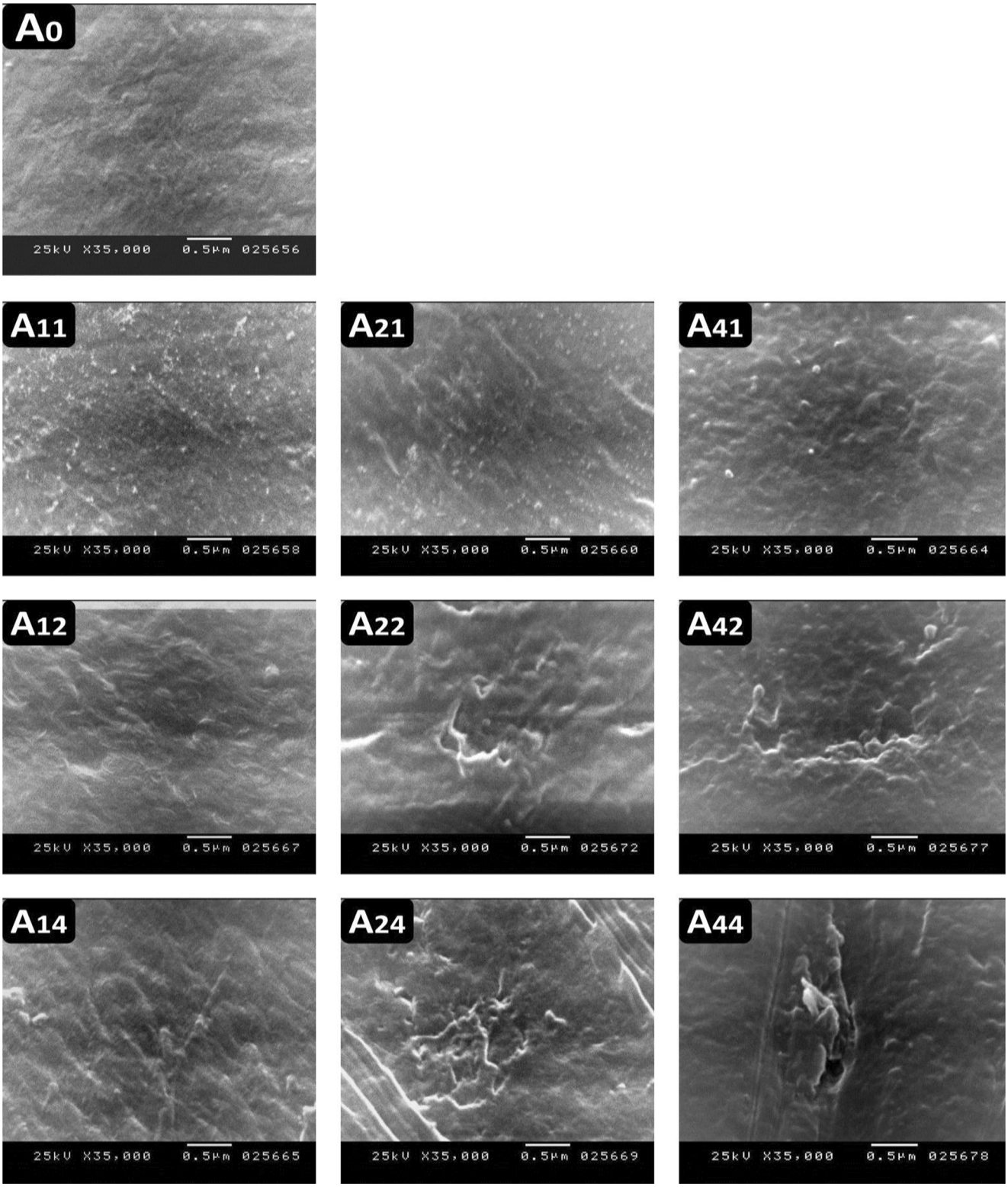

Fig. 2 SEM images of surfaces HDPE/PBS/NPCC nanocomposites samples

which leads to cavities, micro-cracks, micro-voids, interface debonding and causes plastic deformation for the HDPE matrix with stress concentration that was formed around NPCC particles becoming weak spots in the polymer matrix and affecting all the mechanical and physical properties of HDPE composites [15–17, 29]. As shown in Fig. 3, there was no clear evidence on the occurrence of phase separation between HDPE and PBS, this homogeneity might be due to

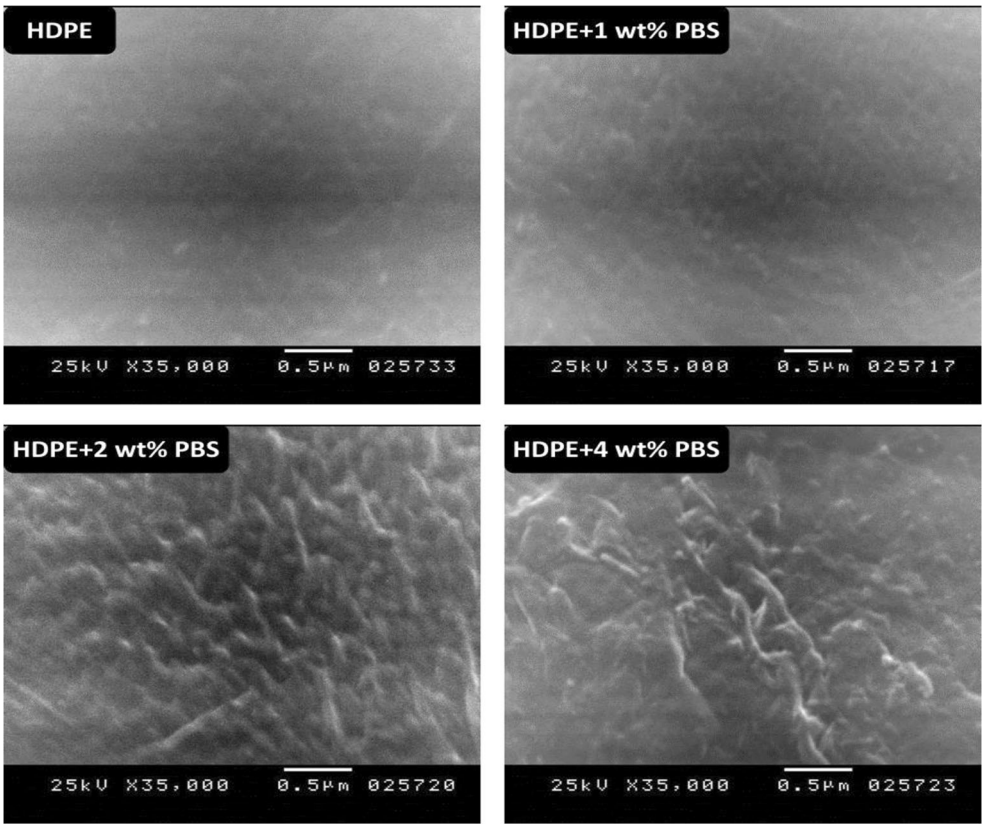

Fig. 3 SEM images of the cross sectional area of HDPE samples that contains 1, 2, 4 wt% PBS to investigate their miscibility, in addition to neat HDPE sample as a reference

using small weight percentages of PBS, using higher percentages would require adding a compatibilizer to solve the immiscibility problem [30].

Chemical structure as investigated by Fourier transform infrared spectroscopy (FTIR)

FTIR spectroscopy was used to investigate the existence of different functional groups of the components of HDPE, PBS, and NPCC composites and if a kind of interaction between these components has occurred. The FTIR spectra of neat HDPE A0, A11, A22, and A44 are shown in Fig. 4. The FTIR spectrum of neat HDPE showed the presence of 4 major peaks at 2995 cm^{-1} for (CH_2) asymmetric stretching vibration, 2869 cm^{-1} for (CH_2) symmetric stretching vibration, 1457 cm^{-1} for (CH_2) bending vibration, 727 cm^{-1} for (CH_2) rocking bending vibration. A new peak appeared at 874 cm^{-1} due to (C-O) bending vibration of the NPCC, which was not apparent in the FTIR spectrum of neat HDPE. Moreover, the FTIR characteristic peaks of neat HDPE at (1454 and 1472)cm^{-1} were shifted to (1431 and 1460) cm^{-1}, this shift may be due to the interaction between HDPE and NPCC [31]. Stearic acid-modified NPCC exhibited the peaks at 2994 cm^{-1} and 2868 cm^{-1}, which are attributed to stearic acid traces on the surface of the NPCC and had the same frequencies as those of pure stearic acid [15]. The absorption FTIR spectra of neat HDPE and HDPE+ 1 wt% PBS, and PBS have characteristic groups like ester carbonyl groups (C=O) stretching vibration at 1721 cm^{-1}, 2994 cm^{-1} for (CH_2) asymmetric stretching vibration and weak absorption at 3436 cm^{-1} assigned to chain-end hydroxyl groups [32, 33].

Mechanical properties of the nanocomposites of the HDPE/ PBS and NPCC

In order to study the effect of adding calcium carbonate nanoparticles (NPCC) and polybutylene succinate (PBS) to the HDPE matrix on the mechanical properties and assess the improvement. The mechanical analyses were conducted on the composites samples while the tensile strength at yield and the elongation percentage at break were recorded.

Tensile strength at yield

The tensile strength at yield or (yield strength) of the HDPE/ PBS/ NPCC composites showed almost no significant change at low loadings of NPCC whether the samples contained PBS or not in the HDPE composites (Table 2). The yield strength of the polymeric composites is usually to be influenced by the inorganic nano-filler dispersion in the matrix due to the increase of the surface contact area of the nanoparticles and interaction or interfacial adhesion between the nano particles and HDPE matrix. Therefore, when the HDPE matrix was filled with a low wt% of treated NPCC with a size less than

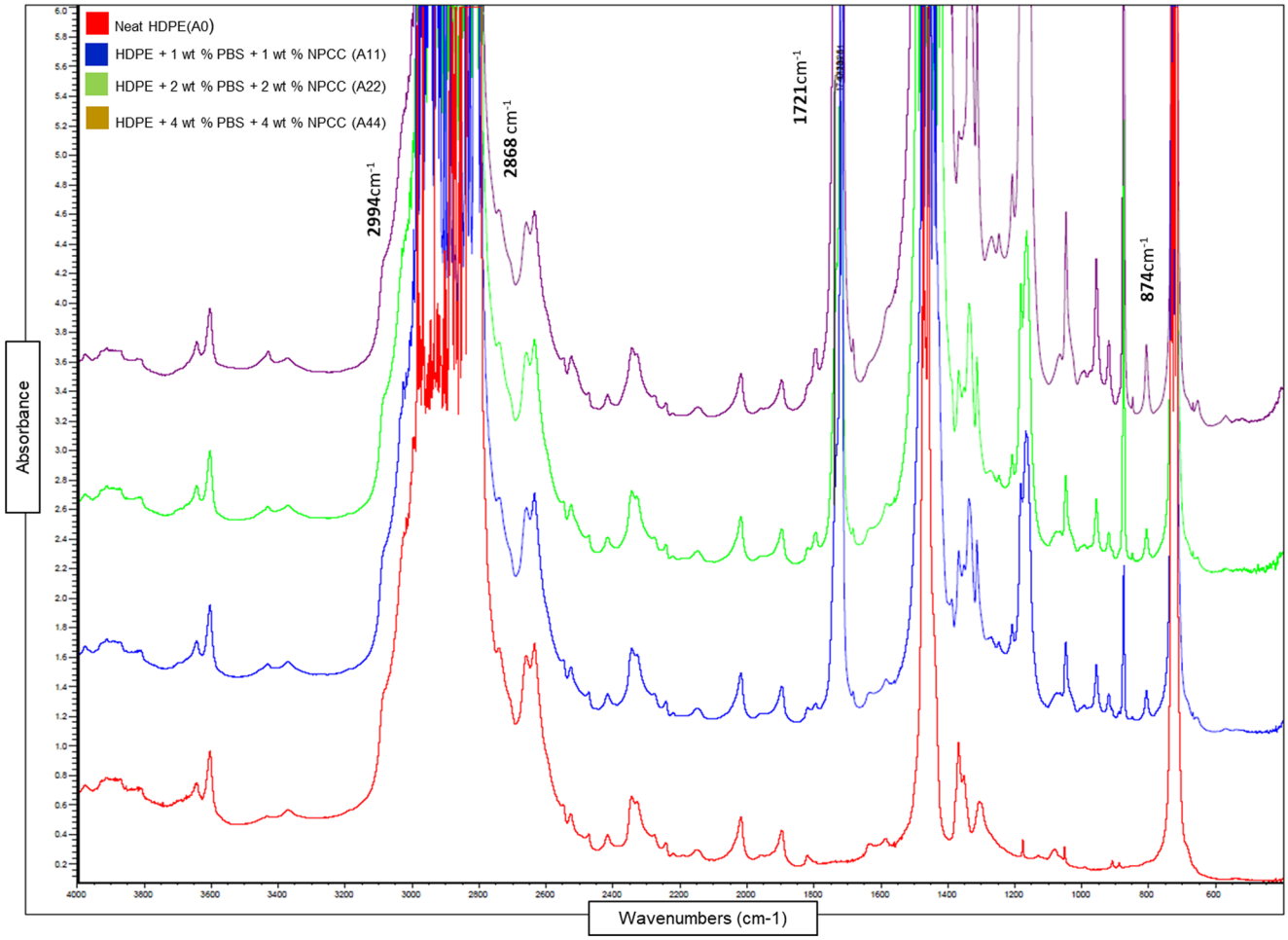

Fig. 4 FTIR spectra of neat HDPE (A0) and HDPE/PBS/NPCC nanocomposites (A11, A22, and A44) samples

100 nm, the nanoparticles were homogenously dispersed in the HDPE matrix resulting in a very large surface area and large contact area with HDPE. Moreover, the interfacial interaction between the treated NPCC and the HDPE matrix is strong even without a compatibilizer [15, 16, 20, 34, 35]. Raising the NPCC weight percentage in the HDPE matrix did not have much influence on the tensile strength of the nanocomposite. It has been reported that the yield strength would not be significantly affected by a few nanoparticles agglomerates because the yield strength is a low-strain property which means that it is measured at yield before any significant plastic deformation occurs. At low-strain zone, the adhesion between the matrix and NPCC remains constant and resists the plastic deformation due to the rigid nature of NPCC which restricts the molecular mobility inside the HDPE matrix. Consequently, the tensile strength didn't excessively decrease as was expected [34].

On the other hand, the tensile strength at yield has decreased by adding PBS and by raising its content in the composites (Table 2). This observation was reported previously in many research articles [15, 31, 36]. This yield strength reduction indicates a poor interfacial adhesion between the phases of HDPE and PBS; the blend of HDPE and PBS is an immiscible blend as the HDPE is nonpolar matrix while PBS is polar one. That is why the distribution of PBS in the HDPE matrix was not uniform which resulted in a weak interfacial adhesion and high interfacial tension between both phases. Moreover, The PBS matrix has a ductile nature with a low yield strength which could be considered one more reason for the composites yield strength reduction after the incorporation of PBS. Additionally, PBS has lower crystallinity than HDPE which might contribute to the reduction of the composites yield strength [12, 32].

Elongation at break (%)

The elongation at break was improved by 35% after incorporating 1 wt% of NPCC, it increased from (1085% for A0) to (1398% for A11), Fig. 5 and (1319% for A01), which proves that the NPCC played the main role of the elongation percentage enhancement. The elongation percentage at break describes and correlates the toughening effect mechanism with the occurrence of NPCC debonding inside the HDPE matrix [37].

Generally, the usage of nano rigid fillers like NPCC increases the polymers toughness, but the theories that explain

Table 2 Tensile properties of HDPE loaded with different percentages of PBS and NPCC

Samples	Tensile Strength (MPa) ± Standard deviation	Elongation at break (%) ± Standard deviation
A0	$26.0^{a} \pm 0.0$	$1084.7^{b} \pm 13.9$
A01	$26.0^{ab} \pm 1.0$	$1319.0^{a} \pm 7.0$
A02	$26.0^{ab} \pm 0.0$	$1261.7^{a} \pm 26.8$
A04	$26.0^{ab} \pm 0.0$	$1255.3^{ab} \pm 32.1$
A11	$26.0^{ab} \pm 1.0$	$1398.3^{ab} \pm 12.1$
A12	$26.0^{ab} \pm 0.0$	$1349.0^{ab} \pm 25.2$
A14	$26.0^{ab} \pm 1.0$	$1248.3^{ab} \pm 62.7$
A21	$25.3^{ab} \pm 0.6$	$1298.0^{ab} \pm 43.7$
A22	$25.7^{ab} \pm 0.6$	$1219.0^{ab} \pm 5.2$
A24	$25.7^{ab} \pm 0.6$	$1211.0^{ab} \pm 31.0$
A41	$25.0^{b} \pm 0.0$	$1234.0^{ab} \pm 12.5$
A42	$25.7^{ab} \pm 0.6$	$1151.3^{ab} \pm 20.6$
A44	$25.7^{ab} \pm 0.6$	$1029.7^{b} \pm 13.1$
F (p)	2.701^{*} (0.029^{*})	3.644^{*} (0.007^{*})

Elongation at break % is statistically significant (*P* Value <0.05)

F F for ANOVA test

p p value for comparison between the different studied groups.

*: Statistically significant at $p \leq 0.05$

Means with Common letters are not significant (i.e. means with different letters are significant).

Data was expressed using Mean ± SD

the polymers toughening were lacking some understanding till the study made by Argon et al. [19] who explained the toughness improvement mechanism using rigid filler systems. Lazzeri et al. [20] provided more studies and also investigated the same mechanism of Bartczak, Argon and Cohen. At the high strain zone, in which the plastic deformation occurs, the nanoparticles debond from the polymeric matrix leaving voids and allowing the inter particle ligaments to deform plastically. The stretching of the matrix ligaments between these voids or debonded particles is the main absorbing energy mechanism which can delay the sample fracture.

The key of improving toughness and increasing elongation is how to control the debonding effect (voids formation) to favor debonding and the interfacial property between the NPCC in HDPE matrix. By loading the suitable weight percentage (at low wt%) of NPCC which is able to distribute itself homogenously and appropriately adhere to the HDPE matrix, adequate adhesion is essential to prevent the particles agglomeration and avoid the voids coalescence (cavities and micro cracks) which act as weak points and stress concentrators (fraction initiation) in the polymer matrix. On the other hand, the adhesion between the particles and the matrix should not be very strong to favor debonding from the matrix at high strain and form suitable number of voids around the particles to stretch and absorb the energy [19, 20, 38]. Also, the treatment of NPCC with stearic acid would contribute to a good dispersion of the particles as it reduces the particle–particle interaction, which will lead to better particles dispersion in the HDPE matrix. Moreover, it can reduce the polymer–particle adhesion, and this has consequences on the debonding effect occurring in the HDPE/NPCC composite. When the adhesion is medium, the debonding mechanism becomes more operative and the plastic deformation of the HDPE matrix enhances. Also, at the high strain zone, NPCC alters the stress state in the HDPE around the particles which acts as a lubricant and promotes for a better molecular mobility in the polymeric matrix when stress is applied and induces extensive elongation in the matrix as shown in Fig. 6 [5, 15–18, 28, 29, 39]. Similar observation of the stretching flow of NPCC composites at low wt% has been reported in other studies [15, 29, 39].

By increasing the NPCC wt%, the elongation at break % decreased as shown in Figs. 7 and 8. At higher wt% of NPCC, the nanoparticles agglomeration occurred as clearly noticed by SEM examination. These agglomerates generate stress concentration around the nanoparticles of $CaCO_3$, leave large voids, initiate cracks, debonding stress in polymer's chains which lead to cracks growth and decrease the elongation at break % [15, 29, 31, 35, 36]. Also increasing the PBS wt% in the HDPE matrix resulted in a reduction in the elongation percentage at break. It should be noted that HDPE is a non-polar polymer but PBS is a polar polymer, that's why they are immiscible components. For two immiscible polymers, the distribution of PBS is not uniform and the interfacial adhesion is weak due to the high interfacial tension inside the composite system. Consequently, the elongation at break % becomes worse [30].

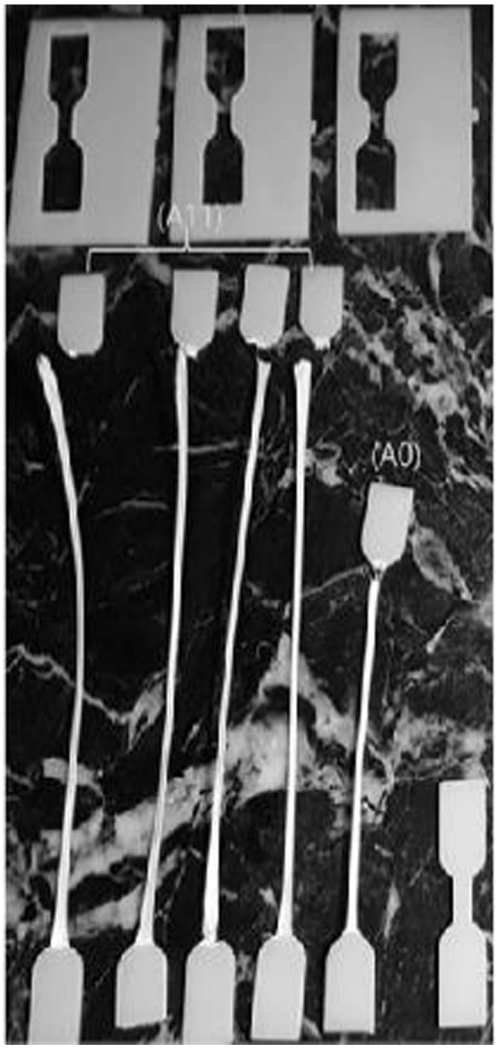

Fig. 5 The improving in elongation at break (%) for (A11) compared to the (A0)

Impact strength

Izod impact test shows the resistance and toughness of materials which is a factor of its ability to absorb energy during plastic deformation. The results of impact strength of the prepared nanocomposites were presented in Table 3 and showed an increase in HDPE composites impact toughness which consists of 1 wt% of NPCC. Several studies have demonstrated an increase in toughness of the polymer matrix using a suitable concentration of rigid particles such as NPCC. The reinforcement of high density polyethylene with NPCC increases the impact strength by altering the micro mechanism of deformation from crazing and tearing in HDPE matrix to fibrillation in HDPE/NPCC nanocomposite which may be attributed to the strong interaction between HDPE and NPCC. Generally, in the inorganic nanoparticles-reinforced in semi-crystalline thermoplastic materials, the micro deformation processes that have been identified as energy dissipating mechanisms include cavitation or debonding of minerals with consequent microvoid formation and deformation bands. So, the micro-void combines and bridges the matrix elements to form a stretched fibril (fibrillation). The extensive fibrillation releases the plastic constraint in the matrix, resulting in a large-scale plastic deformation with the consequent extension of matrix ligaments, and stretching of fibrils as shown in Fig. 9 [5]. However, with the increase of NPCC amount, the impact strength of the composites decreases, which may be due to the agglomeration occurring among NPCC particles. The interfacial compatibility also became worse, and that led to the decrease of impact strength [15, 16, 40]. On the other hand, the impact strength of the HDPE/PBS/NPCC composites was decreased with increasing the wt% of PBS in the HDPE matrix due to interfacial incompatibility of HDPE and PBS [30].

Thermal properties of the nanocomposites of the HDPE/ PBS and NPCC

Differential Scanning Calorimetry (DSC)

To study the thermal properties of neat HDPE and HDPE/PBS/NPCC composites, Differential Scanning Calorimetry (DSC) analysis has been carried out, which determines, in a quantitative way, the amount of heat absorbed or evolved by a sample [41]. Figure 10 shows the melting part of a typical DSC thermogram of sample A11 which was conducted according to the temperature program described previously in the experimental section. The melting temperature and the degree of crystallinity % of the neat HDPE and each composite are listed in Table 4. The DSC melting curves of the neat HDPE and its composites seemed quite similar. However, the presence of NPCC in the HDPE matrix slightly increased the melting temperature of the HDPE nanocomposites. These results are consistent with several researchers who reported that the addition of NPCC in the HDPE matrix had a major effect in increasing the melting temperature of the samples, this might be due to the flexibility deterioration of the HDPE chains caused by the NPCC particles presence which can restrict the movement of the polymer chain segments and raise the melting temperature of the composites [16, 22, 31, 42–45].

The results in Table 4 show that the degree of crystallinity (%) of the nanocomposite samples decreased from (82.07% for A0) to (79.62% for A11), (76.8% for A14), and (65.12% for A44). The general trend shows that NPCC presence caused a reduction in the degree of crystallinity, which is consistent with what has been reported in other previous researches [31, 43–47]. There are two mutually inverse effects of NPCC on the crystallization behaviour of HDPE nanocomposite that were observed. On one hand, it was expected that the presence of NPCC will enhance the nucleation rate and the

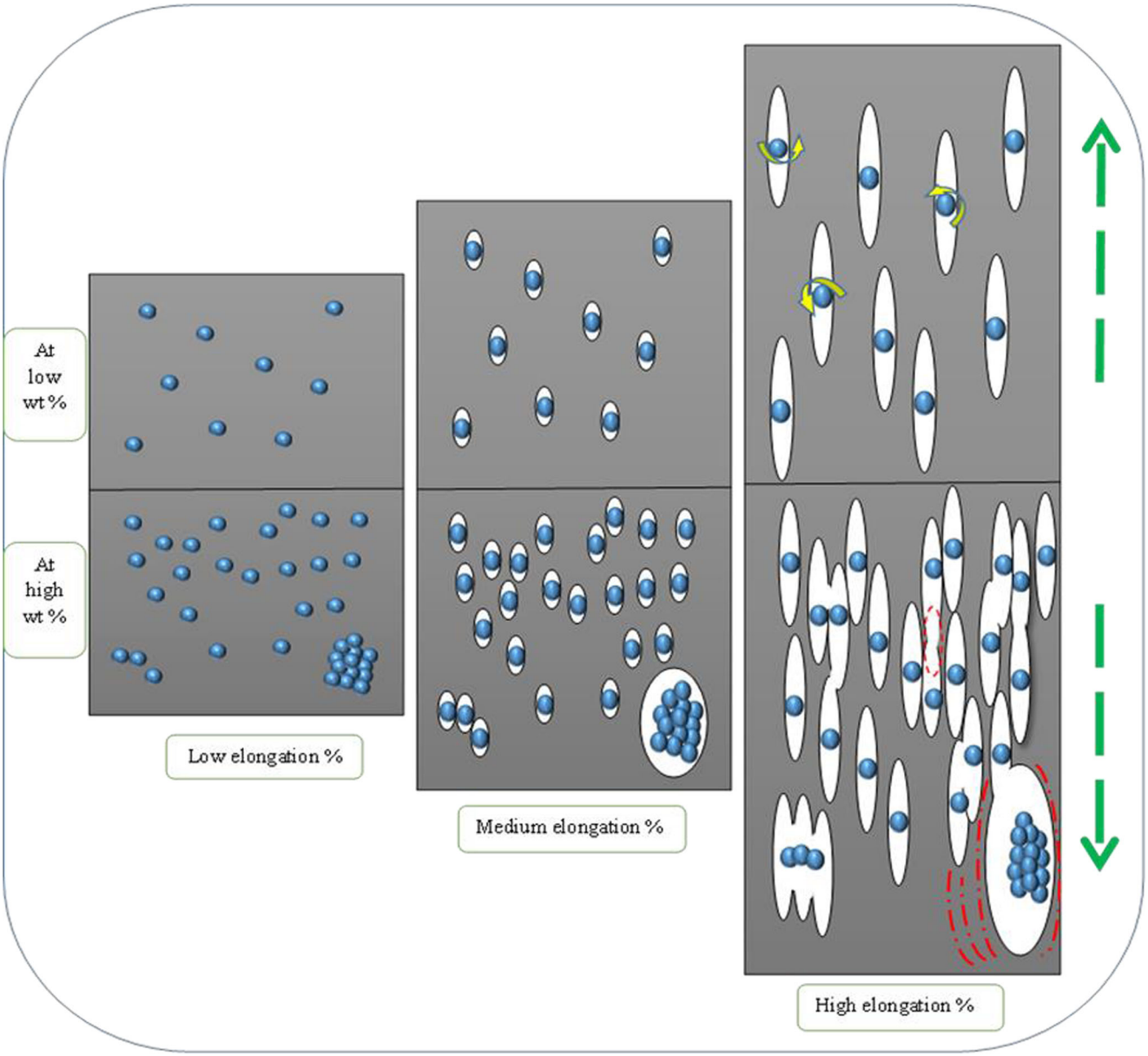

Fig. 6 Toughening effect mechanism with rigid nanoparticles for the polymeric matrix

spherulites growth rate to promote the crystallinity index. But on the other hand, NPCC might have restricted the movement of the HDPE chain segments and shortened the solidification time of the HDPE nanocomposites [45]. Especially HDPE which has fast crystallization rate more than some other polymers such as polypropylene (PP), that's why it's difficult to control its nucleation which led to a heterogeneous nucleation of NPCC in the matrix and accordingly decreased the crystal domain. Furthermore, shrinkage might have occurred in the free volume/spaces that are available to be occupied by NPCC molecules which inhibit the crystal growth and the disturbance of NPCC agglomerates for entrance chains to semi-crystalline cells at high wt% resulting in a reduction in the spherulite growth and possibly asymmetric crystals. The combination of nucleation sites and retarded crystal growth is expected to produce fine size crystals and imperfect spherulites and lead to a reduction in the crystallinity index of the composites [27, 34, 43–46]. This reduction of the crystallinity index means that the heat required to process the nanocomposites during injection molding is reduced, which leads to more power efficiency and money saving [44].

Thermogravimetric analysis (TGA)

Thermogravimetric analysis was used to investigate the thermal degradation behavior of neat HDPE and its nanocomposites in a controlled atmosphere (nitrogen). The thermal stability were studied using parameters such as the Initial

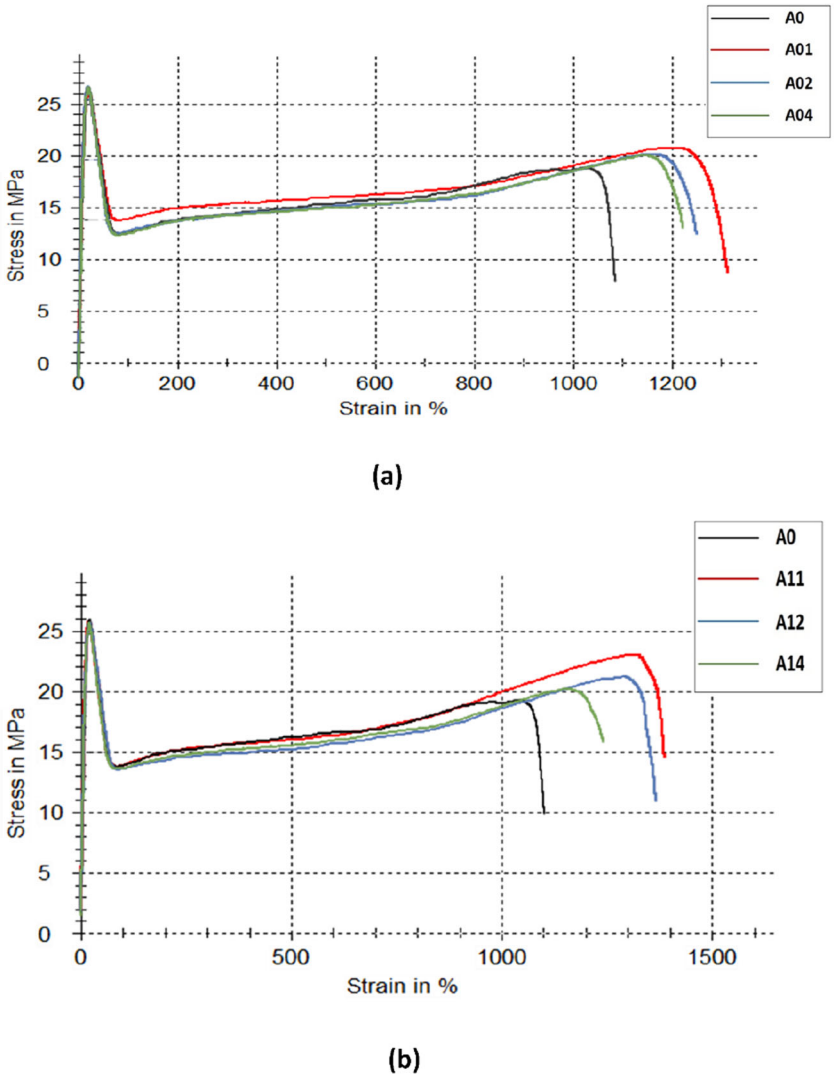

Fig. 7 The effect of different wt% of NPCC in the stress–strain curves of HDPE/PBS/NPCC with **a** 0 wt% of PBS, **b** 1 wt% of PBS

Degradation Temperature (IDT), the temperature at 50% weight loss (D $_{50}$%), and the final residue percentage at 600 °C and were all recorded Table 5. The thermograms of neat HDPE (A0), the HDPE/NPCC nanocomposites (A01, A02 and A04) are shown in Fig. 11a. The thermal decomposition of the neat HDPE sample occurred at a temperature range of (305 °C – 517 °C) with a weight loss of (99.23%). The final residue that was left after the combustion of A0 was very small (0.766%), due to the thermal decomposition of all the organic components into gaseous products [24, 48].

By the addition of NPCC to the HDPE matrix, the Initial Degradation Temperature (IDT) and (D $_{50\%}$) of the HDPE/ NPCC nanocomposite were higher than that of neat HDPE, their values continued increasing by raising the NPCC weight percentage, except for sample A04 which had a slight decrease in the IDT and D $_{50\%}$ values. The residue percentages at 600 °C of HDPE/ NPCC nanocomposites also increased to 1.094%, 2.135% and 4.023% with the addition of (1 wt%, 2 wt% and 4 wt%) NPCC. Accordingly, the introduction of NPCC to the HDPE matrix resulted in an improvement of the thermal stability of the nanocomposite. The NPCC particles might be able to act as a heat barrier earlier during the thermal decomposition process by eliminating the probability of heat permeation into the HDPE matrix and assisting the formation of carbide which prevented the decomposed products volatilization. The slight reduction of (IDT) and D $_{50\%}$ for sample A04 might be due to the agglomeration problem of the inorganic nanoparticles in the organic polymer matrix at higher loadings [42, 43, 48].

Figure 11b shows the TGA thermal curves of HDPE/ PBS/ NPCC nanocomposites (A11, A22 and A44) compared to neat HDPE (A0). As shown in Table 5, there was a slight decrease in the residue percentage, IDT and D $_{50\%}$ after the incorporation of PBS into the HDPE/NPCC nanocomposites. These results indicate a reduction of the nanocomposites thermal stability containing PBS with different loadings. This reduction might be attributed to the behavior of the PBS which experiences a cyclic decomposition mechanism around

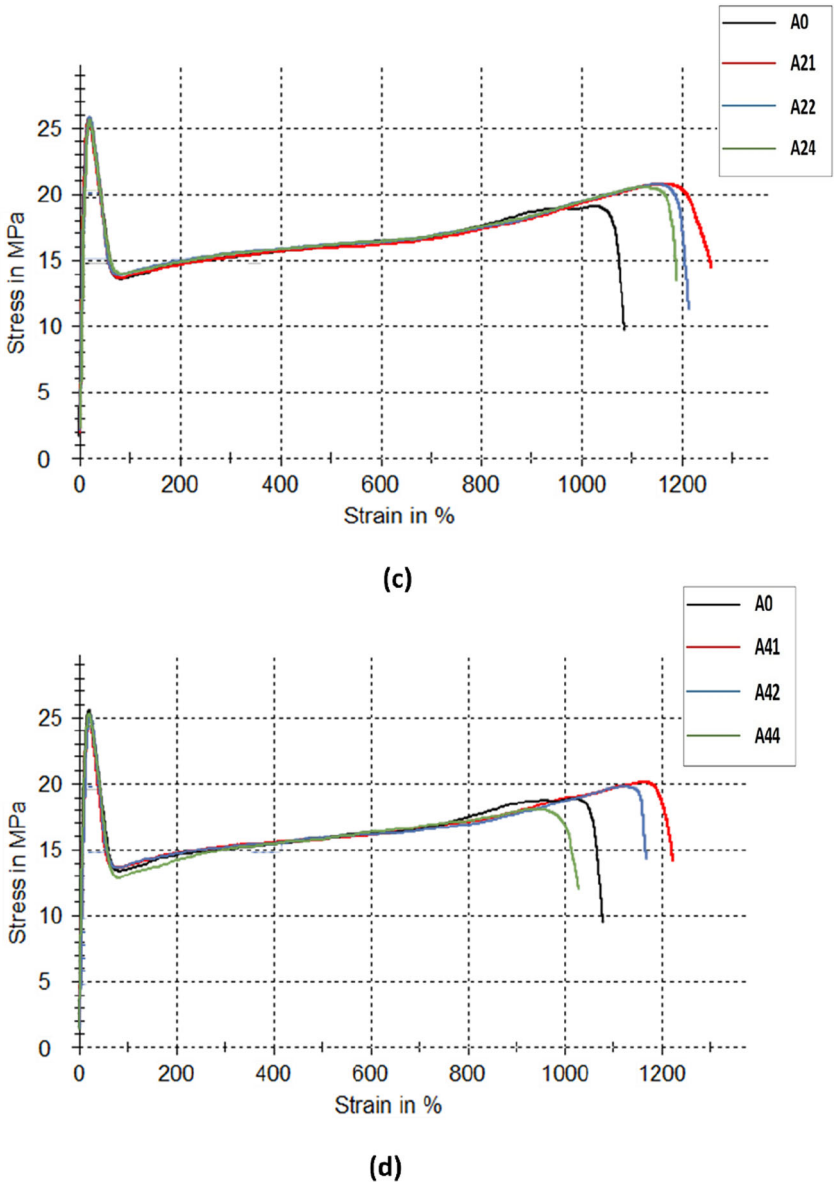

Fig. 8 The effect of different wt% of NPCC in the stress–strain curves of HDPE/PBS/NPCC with **a** 2 wt% of PBS, **b** 4 wt% of PBS

360 °C caused by the breakdown of the ester groups and scission of the C–O and C–C bonds and some of the predominant byproducts such as anhydrides, olefins and carbon dioxide on the polymer backbone [48, 49].

Physical properties of nano composites of HDPE / PBS and NPCC

Melt flow index (MFI)

The melt flow index is an important parameter for characterization of the physical and processing properties of polymeric materials, the change in MFI value indicates a change in motion of the HDPE chains [15]. The melt flow index of the HDPE matrix varied as a function of the NPCC and PBS content as summarized in Table 6. The MFI of the composites has decreased with increasing the wt% of NPCC content, as previously reported in literature [15, 16, 47, 48]. The shear stress and viscosity of the composites were increased when the amount of NPCC in the polymeric composites increased. In general, the incorporation of fillers hinders the plastic flow, increases the viscosity of the polymer melt and reduces the MFI as expected [16]. This reduction of MFI of the composites was related to the reduction in the chains mobility around the nano-filler which decreases the polymer flow through the injection machine die with increasing the NPCC content. Therefore, the polymer processing was affected by the flow properties of the material [16, 47]. Also, the MFI of HDPE/PBS/NPCC composite has increased with increasing the wt% of PBS. The viscosity of the composites decreased with increasing the PBS content which may be due to its high melt flow index. The addition of PBS makes a lubrication

Table 3 The effect of loading different (wt%) of PBS and NPCC to HDPE blend on its impact strength

Samples	Impact strength (kJ/m^2)± Standard deviation
A0	11.78^a ± 0.79
A11	14.77^a ± 0.26
A12	12.70^a ± 2.31
A14	12.35^a ± 2.57
A21	13.60^a ± 0.26
A22	12.45^a ± 2.61
A24	11.18^a ± 1.24
A41	13.01^a ± 1.83
A42	12.20^a ± 3.39
A44	11.00^a ± 0.67
F (p)	1.796 (0.132)

F F for ANOVA test

p p value for comparison between the different studied groups

Means with Common letters are not significant (i.e. Means with Different letters are significant)

Data were expressed using Mean ± SD

*Statistically significant at $p \leq 0.05$

effect for the HDPE matrix, and the flow resistance of the HDPE melts decreases, resulting in a decrease of its viscosity. So, the MFI increases with increasing the PBS content [50].

Whiteness index

Table 7 illustrates the effect of the addition of PBS and NPCC on optical property (whiteness index) of the HDPE /PBS/NPCC composites. The HDPE composites that contains 1 wt% of NPCC has a significant improvement and highest value of whiteness index. The reasons for this behavior may be due to the small particle size, large surface area and high light scattering effect of NPCC. The incident light on HDPE/ NPCC nanocomposite was refracted on air. Also the NPCC showed a mild pigmentary effect in the polymeric matrix [51, 52]. However, by the addition of NPCC more than 1 wt% of the HDPE matrices, the whiteness index decreased. Generally, at the high weight percentage of NPCC, the whiteness index decreased due to the agglomeration of the particles, which makes up the defects of bad dispersion and micro cavities that appear at the interface of two different phases. Also, the whiteness index increased when wt% of PBS increased which may be due to the high whiteness index of PBS, which reduced the composite's yellowness expressed by yellowness index and increased the whiteness index [52, 53].

Biodegradation of plastics

A selected microorganism (Aspergillus oryzae) was allowed to attack HDPE/ PBS/NPCC composites under laboratory conditions to compare the degradability of this composite to the blank neat HDPE. The biodegradation was analyzed by two methods: Determination of the weight loss (%) and examination for the HDPE surfaces by scanning election microscope (SEM). The sample containing only 1 wt% PBS was chosen to test our hypothesis which assuming that the PBS presence will encourage the microorganisms to grow and attach themselves irreversibly to the sample surface and use not only the PBS as a carbon source but also the polyethylene molecules. Minimum load percentage of PBS would indicate the hypothesis accuracy more quickly.

Determination of weight loss %

The effect of biodegradation on the weight loss (%) during the period of 2,4,6 and 8 weeks for neat HDPE blank samples

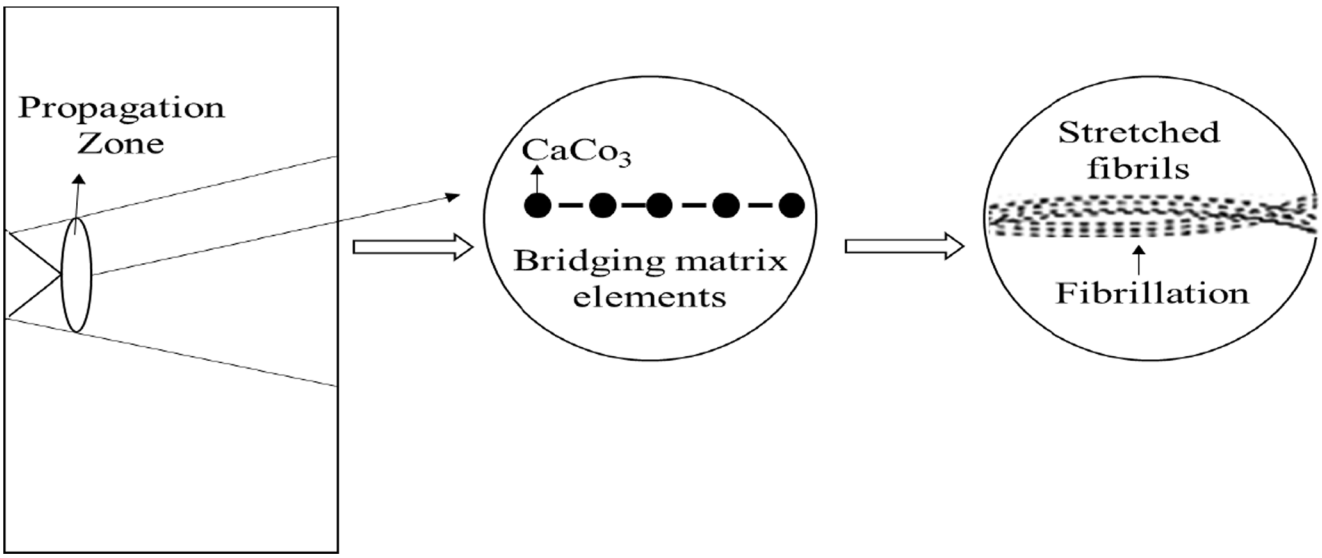

Fig. 9 The fibrillated fracture process in HDPE/NPCC nanocomposite [5]

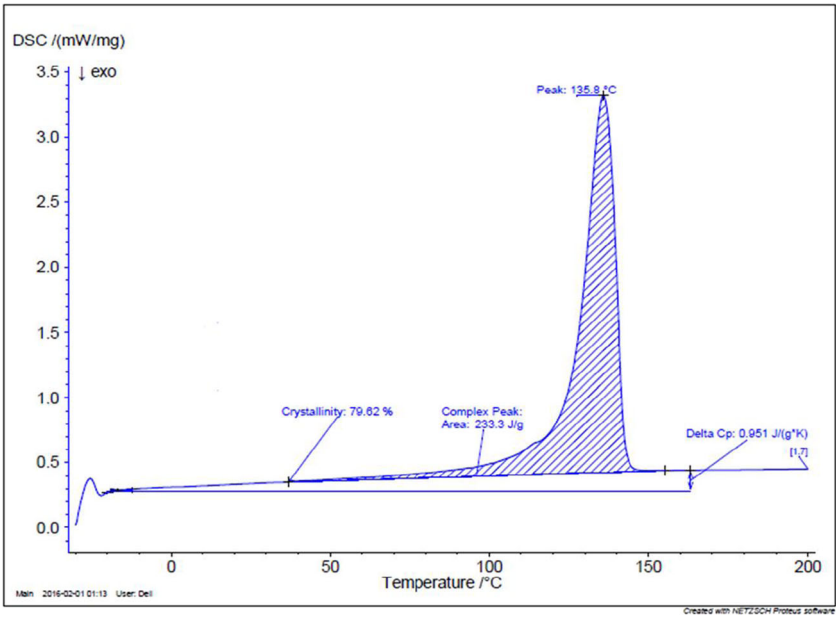

Fig. 10 DSC NETZSCH plot for (A11)

(A0) and HDPE/ PBS/ NPCC composite (A11) samples by fungus *A. oryzae* are shown in Table 8 and Fig. 12. The obtained results showed that the weight loss (%) has increased with time during the degradation of sample (A11) and reached 0.265% after 8 weeks, which may be considered an important indication about the biodegradation process. However, there was no any loss in the weight % of the blank (A0).

These results indicated, that the effect of the presence PBS in the matrix, polybutylene succinate (PBS) was used as a biodegradable additive to high density polyethylene (HDPE) to be the fermentation substrate for the filamentous fungus *Aspergillus oryzae*. It was found that PBS can be degraded by the enzymes of *Aspergillus oryzae*. It is capable of secreting large amounts of enzymes (cutinase L1, α-amylase and gluco-amylase) which are common microbial enzymes involved in the degradation of biodegradable synthetic esters plastics such as PBS, poly-(caprolactone) (PCL), PLA by extra or intracellular depolymerases [54, 55].

The fungus *A.oryzae* attacks HDPE/ PBS/ NPCC composite to obtain the carbon source and therefore the extracellular enzymes are secreted when the strain is grown in a medium containing the composite which utilizes it as a sole carbon source and resulting in a biodegradation of such composite [14, 54, 56].

Microorganisms likely remove all the weaker (hydrolysable) bonds first. These bonds might form during HDPE composite processing, storage, or due to UV degradation by exposure to the sun or including carboxyl groups from PBS loading, peroxide groups and unsaturated bonds. So, long polymer chains of HDPE were likely cut into shorter

Table 4 DSC results of the thermal properties of HDPE/PBS/ NPCC nanocomposite with different weight percentages

Samples	Mean melting temperature Tm (°C) ± Standard deviation	Crystallinity degree Xc (%) ± Standard deviation
A0	$134.3^{g} \pm 0.07$	$82.07^{a} \pm 0.02$
A11	$135.8^{cd} \pm 0.07$	$79.62^{b} \pm 0.01$
A12	$136.0^{bc} \pm 0.07$	$78.47^{c} \pm 0.02$
A14	$135.9^{cd} \pm 0.07$	$76.8^{e} \pm 0.01$
A21	$135.5^{de} \pm 0.07$	$76.61^{f} \pm 0.01$
A22	$136.7^{a} \pm 0.14$	$71.86^{h} \pm 0.01$
A24	$135.3^{ef} \pm 0.21$	$76.93^{d} \pm 0.02$
A41	$136.5^{ab} \pm 0.07$	$72.73^{g} \pm 0.01$
A42	$134.7^{f} \pm 0.14$	$68.92^{i} \pm 0.01$
A44	$135.7^{cd} \pm 0.07$	$65.12^{j} \pm 0.01$
F (p)	86.685^{*} ($<0.001^{*}$) ($<0.001^{*}$)	$2{,}206{,}446.6^{*}$

Table 5 Results of TGA measurements of the neat HDPE and HDPE/NPCC and HDPE/PBS/NPCC nanocomposites

Sample	IDT (°C)	D50% (°C)	Residue at 600 °C (%)
A0	304.98	478.05	0.766
A01	324.32	485.22	1.094
A02	328.08	487.5	2.135
A04	318.08	485.97	4.023
A11	294.11	469.83	1.463
A22	313.16	477.53	2.079
A44	291.34	482.21	3.942

Table 6 The MFI of the HDPE/PBS/NPCC nanocomposites

Samples	MFI (g/10 min) ± Standard deviation
A0	$7.24^{d} \pm 0.1$
A11	$7.31^{d} \pm 0.0$
A12	$7.23^{d} \pm 0.0$
A14	$7.18^{de} \pm 0.1$
A21	$7.79^{bc} \pm 0.0$
A22	$7.56^{d} \pm 0.0$
A24	$7.29^{e} \pm 0.0$
A41	$7.97^{a} \pm 0.0$
A42	$7.84^{ab} \pm 0.0$
A44	$7.69^{c} \pm 0.0$
F (p)	127.523^{*} ($<0.001^{*}$)

* Statistically significant (*P* Value <0.05)

pieces due to the action of enzymes secreted by microorganisms [57]. Figure 13 shows the common mechanism of biodegradation of the plastics such as HDPE through the microbial enzymes. Firstly, the microorganism such as *Aspergillus oryzae* can produce hydrolytic enzymes in the form of enzyme mixtures – cocktails which adhere to the surface of the HDPE/PBS/ NPCC composite (and called biofilm) as shown in Fig. 14, and then, the enzymes catalyze a hydrolytic cleavage of the chains from the carboxyl end of the PBS in the polymeric matrix, and dramatically facilitates the PBS composite

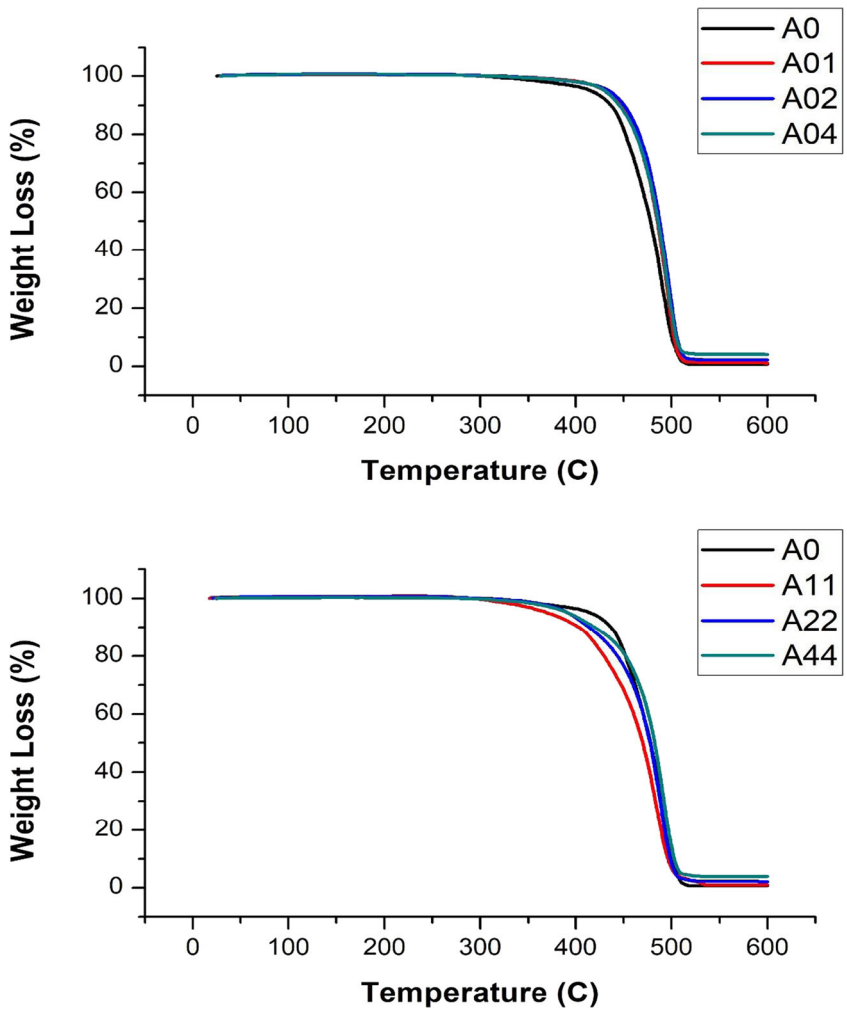

Fig. 11 TGA thermograms of neat HDPE (A0) and **a** HDPE/NPCC nanocomposites **b** HDPE/PBS/ NPCC nanocomposites (the illustration was performed using OriginPro 8)

Table 7 The effect of the NPCC and PBS in HDPE on the whiteness index of the HDPE/PBS/NPCC composites

Samples	White Index ± Standard deviation
A0	$60.2^{e} \pm 0.0$
A11	$67.3^{b} \pm 0.0$
A12	$48.4^{h} \pm 0.0$
A14	$40.3^{i} \pm 0.0$
A21	$66.2^{c} \pm 0.1$
A22	$62.1^{d} \pm 0.1$
A24	$57.3^{g} \pm 0.0$
A41	$68.4^{a} \pm 0.1$
A42	$66.1^{c} \pm 0.0$
A44	$58.4^{f} \pm 0.1$
F (p)	$115{,}780.272^{*}$ ($<0.001^{*}$)

* Statistically significant (*P* Value <0.05)

degradation [58]. The strips therefore become fragile and lose some weight which initiate a preliminary stage of microbial decomposition consisting of a reduction in molecular weight of the composites [57]. Then, the composite disintegrates into short chains of oligomers, monomers which act as a source of carbon and energy to the microorganism. Interestingly, this process is referred to "depolymerisation", whereas mineralization, in which the end products are carbon dioxide (CO_2), water (H_2O) or methane (CH_4) [14, 56, 59, 60].

The chemical structure (responsible for functional group stability, reactivity, hydrophylicity and swelling behavior) and the degree of crystallinity, are the major factors for the rate of degradation of PBS composites. So it can be noted from the differential scanning calorimetry (DSC) experiment, that the decrease in the degree of crystallinity of the samples by adding PBS encouraged an effective biodegradation of the HDPE composite. It is known that the less crystalline region can be more degradable than the crystalline region due to the molecular-chain flexibility and mobility [14, 33, 57, 59]. Also, by mixing the HDPE matrix with polar additives such as PBS/ NPCC, it leads to a decrease in the hydrophobicity and an increase in the hydrophilicity and thus enhance the biodegradation rate of the composite [33]. Also, it can be noticed that, there is no weight loss in the sample (A0) which could be attributed to the neat HDPE resistance to any biodegradation by the microbial attack results from the highly stable C-C and C-H covalent bonds as well as the high molecular weight and its hydrophobic nature [14].

The examination of scanning electron microscope

The SEM examination showed how the fungi *Aspergillus oryzae* can grow on the surfaces of the samples of neat HDPE (A0) and HDPE/ PBS/ NPCC composite (A11) to degrade it after 8 weeks of biodegradation in liquid medium as shown in (Fig. 14a–c).

It can be seen in Fig. 14a that there is no appearance of holes or fungal growth in sample A0, and this could be attributed to the HDPE resistance for the biodegradation and the microbial growth on its surface. On the other hand, as shown in Fig. 14b of sample A11, a number of holes are found on the surface of the sample A11. Figure 14c focused on one of the holes which degraded in the surface of the HDPE/ PBS/ NPCC composite. These holes and cracks show how the fungus can attack HDPE/ PBS composite at the edges as well as the center of the samples. Figure 14d shows that the fungus has a good growth in the surface of A11, which attacks the surface to reach the polyester group of PBS and the HDPE surface to have a carbon source, on a solid substrate, as the growing hyphae of filamentous fungi penetrates the enzymatically modified solid substrate by extension and branching of the growing hyphal tips and in liquid culture fermentation. Hence the secreted proteins are released into the culture medium, resulting in substrate degradation in the whole culture [61]. On the surface of the film that is mounted on networks of hyphae and in the presence of breaks and holes, the fungal mycelia gradually spreads and covers the surface of the composite film as was observed in previous study [21] with a slight modification for filamentous fungi which exists in soil. The growth of gray-colored mycelia of *Aspergillus oryzae* on the surface of HDPE discs is shown in (Fig. 14d, e), producing breaks and small holes on the disc along the direction of its hyphal growth as shown in [Fig. 14(b, c and d)]. The fungi found a suitable substrate which contains a good carbon source from PBS or the short carbon bonds of the HDPE which encourages them to grow and spread their spores on the surface and the secret their enzymes, which were immobilized in the substrate during the surface cultivation. Consequently, their hydrolytic activity is limited to the substrate in the close vicinity of the spreading hyphae. Figure 14g–i) shows the growth of *Aspergillus*

Table 8 Comparison between the different studied groups according to weight loss%

	2 week ($n=2$)	4 week ($n=2$)	6 week ($n=2$)	8 week ($n=2$)	*F*	*p*
Weight loss (%)	0.136 ± 0.001	0.195 ± 0.008	0.251 ± 0.001	0.265 ± 0.003	400.890^{*}	$<0.001^{*}$
Sig. bet. Grps.	$p_1 = 0.001^{*}$, $p_2 < 0.001^{*}$, $p_3 < 0.001^{*}$, $p_4 = 0.001^{*} p_5 < 0.001^{*} p_6 = 0.081$					

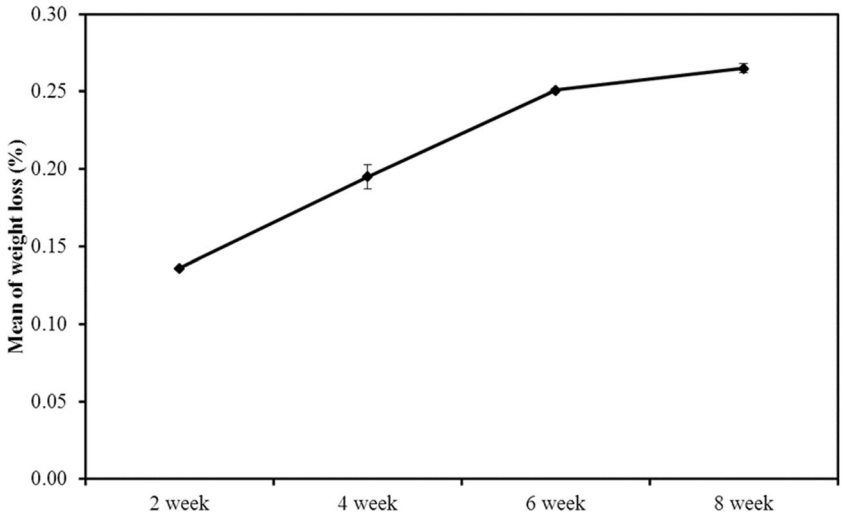

Fig. 12 The weight loss of samples (A0, A11) by the microbial degradation over 8 weeks

oryzae on PDA. It is noted that the spores of *A. oryzae* are the same as that found on the surface of the samples (A11). Generally, the observations of SEM and the results of weight loss (%) support our assumption that the fungus *Aspergillus oryzae* has the ability to secrete enzymes like cutinase (L1), amylase which play an important role in the biodegradation of the PE composites that was explained by (Albertsonn et al., 1987) and also mentioned by (Leja K et al., 2010), and confirm the PBS ability to encourage the fungi to biodegrade the non-biodegradable PE [6, 14, 21, 25, 54, 60, 61].

Conclusions

High density polyethylene (HDPE), polybutylene succinate (PBS) and nano-sized calcium carbonate (NPCC) nanocomposites were prepared using a sequence of injection molding processes. Based on the results obtained, addition of a limited amount of NPCC (1 wt%) to HDPE matrix containing PBS (1 wt%) can lead to the improvement of the mechanical, thermal, physical, morphological properties of the HDPE/PBS/NPCC nanocomposite. The best dispersion of NPCC in the different composites was at 1 wt% that was proved by SEM analysis. More than 1 wt% of NPCC tends to agglomerate and form voids and damages the surface of HDPE matrix. NPCC of 1 wt% increased toughness of the polymer matrix as reflected in higher elongation at break by 35% of the A11 and decreased with increasing of both NPCC and PBS. This indicates a lubricating effect of NPCC during the deformation of the polymer samples. The tensile strength of A11 was nearly the same as A0, and it decreased with increasing the wt% of both NPCC and PBS. The impact strength of HDPE increased by 25.6% for the A11 and decreased with increasing of both NPCC and PBS. The melt flow index of the HDPE/PBS/NPCC composites has decreased with increasing the wt% of the NPCC and increased with increasing the wt% of PBS. The thermal analysis showed that, the melting temperature decreased with increasing the wt% of the NPCC and the Crystallinity degree Xc (%) decreased by the addition of NPCC and PBS. Thermogravimetric analysis (TGA) showed that the thermal stability increased with increasing the weight percentage of NPCC. The sample containing only 1 wt% of PBS was proved to be affected significantly by the microbial attack to give 0.265% weight loss after 8 weeks, compared to the neat HDPE sample which gave 0 wt% weight loss. This indicated the ability of even the smallest weight percentages of a hydro-biodegradable polymer such as PBS when contained in a non-biodegradable matrix, to encourage the microorganism to attach themselves to the substrate and trick them to find a carbon source in the non-biodegradable

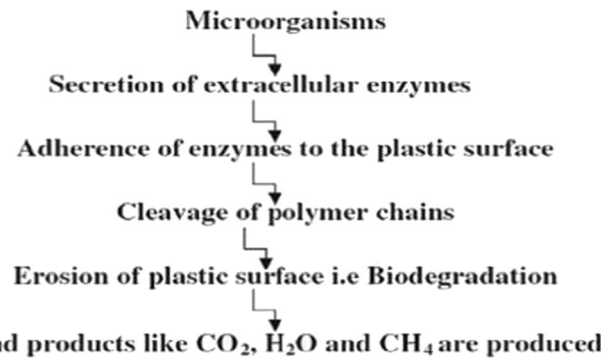

Fig. 13 Mechanism of enzymatic biodegradation of plastic

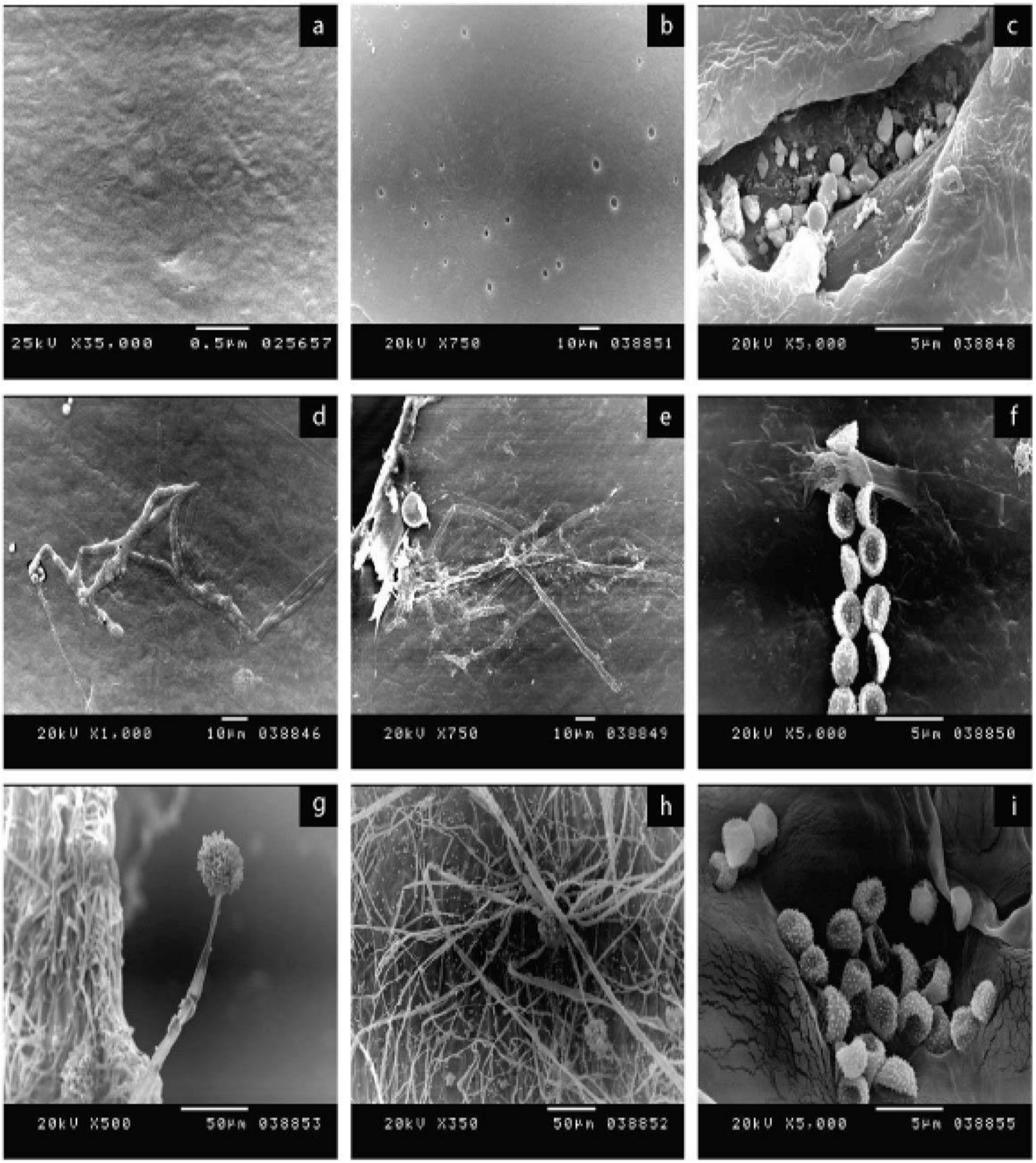

Fig. 14 Scanning electron micrograph of the surface of neat HDPE (A0) and HDPE composite (A11) after degradation by *Aspergillus oryzae* in the liquid medium at 28 ± 1 °C and 120 rpm: **a** Neat HDPE (A0), **b** HDPE biocomposite with holes by fungus, **c** Zoom on one of holes on the surface of (A11), **d** Aspergillus oryzae on the surface of the sample (A11), **e** Growth of Aspergillus oryzae on the surface of the sample (A11), **f** The spores of Aspergillus oryzae on surface of the sample (A11), **g** Shape of Aspergillus oryzae on the Potato Dextrose Agar (PDA), **h** Aspergillus oryzae and its network of hyphae on the (PDA), **i** Spores of Aspergillus oryzae on the (PDA)

polymer (HDPE). This study is considered as a beginning of a scientific and industrial research that is able to develop biodegradable polymer grades out of the traditional non-biodegradable high density polyethylene.

References

1. Ahmadi M, Behzad T, Bagheri R, Heidarian P (2018) Effect of cellulose nanofibers and acetylated cellulose nanofibers on the properties of low-density polyethylene/thermoplastic starch blends. Polym Int 67(8):993–1002
2. Muthuraj R, Misra M, Mohanty AK (2018) Biodegradable compatibilized polymer blends for packaging applications: a literature review. J Appl Polym Sci 135(24):45726
3. Madhu G, Bhunia H, Bajpai PK, Nando GB (2016) Physico-mechanical properties and biodegradation of oxo-degradable HDPE/PLA blends. Polymer Sci Ser A 58(1):57–75
4. Carraher Jr CE (2016) Carraher's polymer chemistry. CRC, Florida
5. Yuan Q, Shah JS, Bertrand KJ, Misra RDK (2009) On processing and impact deformation behavior of high density polyethylene (HDPE)–calcium carbonate Nanocomposites. Macromol Mater Eng 294(2):141–151
6. Albertsson A-C, Andersson SO, Karlsson S (1987) The mechanism of biodegradation of polyethylene. Polym Degrad Stab 18(1):73–87
7. Orr IG, Hadar Y, Sivan A (2004) Colonization, biofilm formation and biodegradation of polyethylene by a strain of Rhodococcus ruber. Appl Microbiol Biotechnol 65(1):97–104
8. Tribedi P, Sil AK (2013) Low-density polyethylene degradation by Pseudomonas sp. AKS2 biofilm. Environ Sci Pollut Res 20(6): 4146–4153
9. Ohtaki S, Maeda H, Takahashi T, Yamagata Y, Hasegawa F, Gomi K, Nakajima T, Abe K (2006) Novel hydrophobic surface binding protein, HsbA, produced by Aspergillus oryzae. Appl Environ Microbiol 72(4):2407–2413
10. Dussud C, Hudec C, George M, Fabre P, Higgs P, Bruzaud S, Delort A-M, Eyheraguibel B, Meistertzheim A-L, Jacquin J (2018) Colonization of non-biodegradable and biodegradable plastics by marine microorganisms. Front Microbiol 9:1571
11. Kannahi M, Rubini K (2012) Biodegradation of polythene bag by Aspergillus oryzae. Biosci Biotechnol Res Asia 9(1):423–426
12. Xu J, Guo B-H (2010) Microbial succinic acid, its polymer poly (butylene succinate), and applications. Plastics from bacteria. Springer, New York, pp 347–388
13. Stevens C (2013) Bio-based plastics: materials and applications. Wiley, New Jersey
14. Leja K, Lewandowicz G (2010) Polymer biodegradation and biodegradable polymers—a review. Pol J Environ Stud 19(2):255–266
15. Sepet H, Tarakcioglu N, Misra R (2016) Determination of the mechanical, thermal and physical properties of nano-CaCO3 filled high-density polyethylene nanocomposites produced in an industrial scale. J Compos Mater 50(24):3445–3456
16. Zaman HU, Beg M (2014) Effect of CaCO3 contents on the properties of polyethylene nanocomposites sheets. Fibers Polym 15(4): 839–846
17. Hu J, Wang Z-W, Yan S-M, Gao X-Q, Deng C, Zhang J, Shen K-z (2012) The morphology and tensile strength of high density polyethylene/nano-calcium carbonate composites prepared by dynamic packing injection molding. Polym-Plast Technol Eng 51(11): 1127–1132
18. Bartczak Z, Argon A, Cohen R, Weinberg M (1999) Toughness mechanism in semi-crystalline polymer blends: II. High-density polyethylene toughened with calcium carbonate filler particles. Polymer 40(9):2347–2365
19. Argon A, Bartczak Z, Cohen R, Muratoglu O (2000) Experimental studies-7 novel mechanisms of toughening semi-crystalline polymers. ACS symposium series, vol 759. American Chemical Society, Washington, DC, pp 98–124
20. Lazzeri A, Zebarjad SM, Pracella M, Cavalier K, Rosa R (2005) Filler toughening of plastics. Part 1—the effect of surface interactions on physico-mechanical properties and rheological behaviour of ultrafine CaCO3/HDPE nanocomposites. Polymer 46(3):827–844
21. Koitabashi M, Noguchi MT, Sameshima-Yamashita Y, Hiradate S, Suzuki K, Yoshida S, Watanabe T, Shinozaki Y, Tsushima S, Kitamoto HK (2012) Degradation of biodegradable plastic mulch films in soil environment by phylloplane fungi isolated from gramineous plants. AMB Express 2(1):40
22. Zebarjad SM, Sajjadi SA, Tahani M, Lazzeri A (2006) A study on thermal behaviour of HDPE/CaCO3 nanocomposites. J Achiev Mater Manuf Eng 17(1–2):173–176
23. Wunderlich B (1980) Chapter IX irreversible melting. Macromolecular physics, vol 3. Academic, New York, pp 128–191
24. Petchwattana N, Covavisaruch S, Chanakul S (2012) Mechanical properties, thermal degradation and natural weathering of high density polyethylene/rice hull composites compatibilized with maleic anhydride grafted polyethylene. J Polym Res 19(7):1–9
25. Sriyapai T, Siripoke S, Chansiri K, Petchwattana N, Somyoonsap P, Mettametha N, Swetwiwathana A, Aungpraphapornchai P, Pothivejkul K, Pringsulaka O (2014) Optimization for production of aliphatic polyester-degrading enzyme from actinomadura sp. strain tf1. Month 30 (2)
26. Raaman N, Rajitha N, Jayshree A, Jegadeesh R (2012) Biodegradation of plastic by Aspergillus spp. isolated from polythene polluted sites around Chennai. J Acad Indus Res 1(6):313–316
27. Zhang Q-X, Yu Z-Z, Xie X-L, Mai Y-W (2004) Crystallization and impact energy of polypropylene/CaCO 3 nanocomposites with nonionic modifier. Polymer 45(17):5985–5994
28. Gao Y, Liu L, Zhang Z (2009) Mechanical performance of nano-CaCO 3 filled polystyrene composites. Acta Mech Solida Sin 22(6): 555–562
29. Homklin R, Hongsriphan N (2013) Mechanical and thermal properties of PLA/PBS co-continuous blends adding nucleating agent. Energy Procedia 34:871–879
30. Aontee A, Sutapun W (2013) Effect of blend ratio on phase morphology and mechanical properties of high density polyethylene and poly (butylene succinate) blend. Adv Mater Res 747:555–559
31. Dastjerdi J, Motlagh EN, Garmabi H (2016) Crystallization, melting, and mechanical behavior of calcium carbonate-based nanocomposites of cross-linked high density polyethylene. Polym Compos 38(1):E402–E411
32. Fan D, Chang PR, Lin N, Yu J, Huang J (2011) Structure and properties of alkaline lignin-filled poly (butylene succinate) plastics. Iran Polym J 20:3–14
33. Mizuno S, Maeda T, Kanemura C, Hotta A (2015) Biodegradability, reprocessability, and mechanical properties of polybutylene succinate (PBS) photografted by hydrophilic or hydrophobic membranes. Polym Degrad Stab 117:58–65
34. Chafidz A, Kaavessina M, Al-Zahrani S, Al-Otaibi MN (2016) Rheological and mechanical properties of polypropylene/calcium carbonate nanocomposites prepared from masterbatch. J Thermoplast Compos Mater 29(5):593–622
35. Khalaf MN (2015) Mechanical properties of filled high density polyethylene. J Saudi Chem Soc 19(1):88–91
36. Cao XV, Ismail H, Rashid AA, Takeichi T (2012) Kenaf powder filled recycled high density polyethylene/natural rubber biocomposites: the effect of filler content. Int J Integr Eng 4(1): 22–25
37. Eiras D, Pessan LA (2009) Mechanical properties of polypropylene/calcium carbonate nanocomposites. Mater Res 12(4):517–522
38. Zuiderduin W, Westzaan C, Huetink J, Gaymans R (2003) Toughening of polypropylene with calcium carbonate particles. Polymer 44(1):261–275
39. Hongsriphan N, Burirat T, Niratsungnern P, Trongteng S (2013) Influence of calcium carbonate nanoparticles on mechanical

behavior of poly (lactic acid)/poly (butylene succinate) blend. J Met Mater Miner 23(1):1–15
40. Wang X, Ming H, Yin H (2015) Fabrication and properties of HDPE/CF/CaCO3/PE-g-MAH quaternary composites. In: IOP Conference Series: Materials Science and Engineering. IOP Publishing, p 012110
41. Guo Q (2016) Polymer morphology: principles, characterization, and processing. Wiley, New Jersey
42. Chrissafis K, Paraskevopoulos K, Pavlidou E, Bikiaris D (2009) Thermal degradation mechanism of HDPE nanocomposites containing fumed silica nanoparticles. Thermochim Acta 485(1):65–71
43. Elleithy RH, Ali I, Ali MA, Al-Zahrani S (2011) High density polyethylene/micro calcium carbonate composites: a study of the morphological, thermal, and viscoelastic properties. J Appl Polym Sci 119(4):2494–2494
44. Chafidz A, Ali I, Mohsin MA, Elleithy R, Al-Zahrani S (2012) Atomic force microscopy, thermal, viscoelastic and mechanical properties of HDPE/CaCO3 nanocomposites. J Polym Res 19(4): 1–17
45. Sahebian S, Zebarjad SM, Khaki JV, Sajjadi SA (2009) The effect of nano-sized calcium carbonate on thermodynamic parameters of HDPE. J Mater Process Technol 209(3):1310–1317
46. Dastjerdi J, Garmabi H (2016) Influence of Nano-sized calcium carbonate on adhesion of HDPE/cross-linked high density polyethylene multilayer structures. Adv Polym Technol 37(3):878–889
47. de Oliveira AG, da Silva ALN, de Sousa AMF, Leite MCAM, Jandorno JC, Escócio VA (2016) Composites based on green high-density polyethylene, polylactide and nanosized calcium carbonate: effect of the processing parameter and blend composition. Mater Chem Phys 181:344–351
48. R-y C, Zou W, H-c Z, G-z Z, Yang Z-t, Jin G, J-p Q (2015) Thermal behavior, dynamic mechanical properties and rheological properties of poly (butylene succinate) composites filled with nanometer calcium carbonate. Polym Test 42:160–167
49. Muthuraj R, Misra M, Mohanty AK (2014) Biodegradable poly (butylene succinate) and poly (butylene adipate-co-terephthalate) blends: reactive extrusion and performance evaluation. J Polym Environ 22(3):336–349
50. Yang J, Qin G, Liang J (2014) Flow properties and extensional viscosity prediction of high-density polyethylene and poly (butylene succinate) blends. J Thermoplast Compos Mater 29(4):479–493
51. DeArmitt C, Hancock M (2003) Filled thermoplastics
52. Liu H, Dong L, Xie H, Wan L, Liu Z, Xiong C (2013) Ultraviolet light aging properties of PVC/CaCO3 composites. J Appl Polym Sci 127(4):2749–2756
53. de Santi CR, Correa AC, Manrich S (2006) Films of post-consumer polypropylene composites for the support layer in synthetic paper. Polímeros 16(2):123–128
54. Maeda H, Yamagata Y, Abe K, Hasegawa F, Machida M, Ishioka R, Gomi K, Nakajima T (2005) Purification and characterization of a biodegradable plastic-degrading enzyme from Aspergillus oryzae. Appl Microbiol Biotechnol 67(6):778–788
55. Dojnov B, Grujić M, Perčević B, Vujčić Z (2015) Enhancement of amylase production using carbohydrates mixtures from triticale in Aspergillus sp. J Serb Chem Soc 80(10):1279–1288
56. Bhardwaj H, Gupta R, Tiwari A (2013) Communities of microbial enzymes associated with biodegradation of plastics. J Polym Environ 21(2):575–579
57. Nowak B, Pająk J, Drozd-Bratkowicz M, Rymarz G (2011) Microorganisms participating in the biodegradation of modified polyethylene films in different soils under laboratory conditions. Int Biodeterior Biodegradation 65(6):757–767
58. Machida M, Yamada O, Gomi K (2008) Genomics of Aspergillus oryzae: learning from the history of Koji mold and exploration of its future. DNA Res 15(4):173–183
59. Chaisu K, Siripholvat V, Chiu C-H (2015) New method of rapid and simple colorimetric assay for detecting the enzymatic degradation of poly lactic acid plastic films. Int J Life Sci Biotechnol Pharm Res 4(1):57–61
60. Li F, Hu X, Guo Z, Wang Z, Wang Y, Liu D, Xia H, Chen S (2011) Purification and characterization of a novel poly (butylene succinate)-degrading enzyme from Aspergillus sp. XH0501-a. World J Microbiol Biotechnol 27(11):2591–2596
61. te Biesebeke R, van Biezen N, De Vos W, Van Den Hondel C, Punt P (2005) Different control mechanisms regulate glucoamylase and protease gene transcription in Aspergillus oryzae in solid-state and submerged fermentation. Appl Microbiol Biotechnol 67(1):75–82